Wood Science and Technology Vol. 9 (1975) p. 243–255

The Light-Gap Technique as a Tool for Measuring Residual Stresses in Bandsaw Blades

By Ricardo O. Foschi
Western Forest Products Laboratory, Vancouver, British Columbia

Abstract. The relationship between residual stress distribution induced in bandsaw blades by cold rolling during tensioning and the transverse deflected shape obtained when the tensioned blade is bent over a given radius is studied. It is shown that the light-gap technique is not a reliable estimator of residual stresses since, while two transverse deflected shapes may be close to each other, the corresponding stress distributions may be far apart. The technique may be improved, within limits, by decreasing the tolerance with which a desired transverse deflected shape is approached during the tensioning process. A method for computing this tolerance is given.

Introduction

To increase bandsaw stability and thus improve sawing accuracy, bandsaw blades are cold rolled to introduce a residual stress distribution with tensile stresses towards the edges of the blade and compressive stresses towards the center. The process is usually known as the "tensioning of the blade" and the stresses introduced are in addition to residual stresses already in the blade and to those created by operation in a bandmill. It is important, therefore, to be able to estimate the magnitude of the residual stresses due to the cold-rolling process, to avoid excessively stressed blades that may exhibit fatigue and gullet cracking problems during operation. Residual stresses are difficult to measure with accuracy by non-destructive means and Szymani and Mote [1974] have presented a review of the different techniques that could be applied to bandsaw blades. Traditionally, saw filers have controlled the level of tensioning in a blade by measuring the "light-gap" when the blade is bent over a certain radius. Fig. 1 shows a tensioned blade, with residual stresses $\sigma_0(y)$, bent over a radius R. Due to the internal stresses σ_0, a transverse curvature is observed and, for example, the straight line AOA becomes the curve $A'O'A'$ when the blade is bent. The ordinate δ of this curve is known as the light-gap, as it is the gap allowing light to pass through the narrow slit between the blade and a straight edge touching both points A'. It has been observed that δ depends upon the number of cold-rolling passes, their location and the pressure used [Aoyama 1970, 1971, 1974]. It has been inferred, therefore, that δ can be used as a measure of the residual stresses introduced.

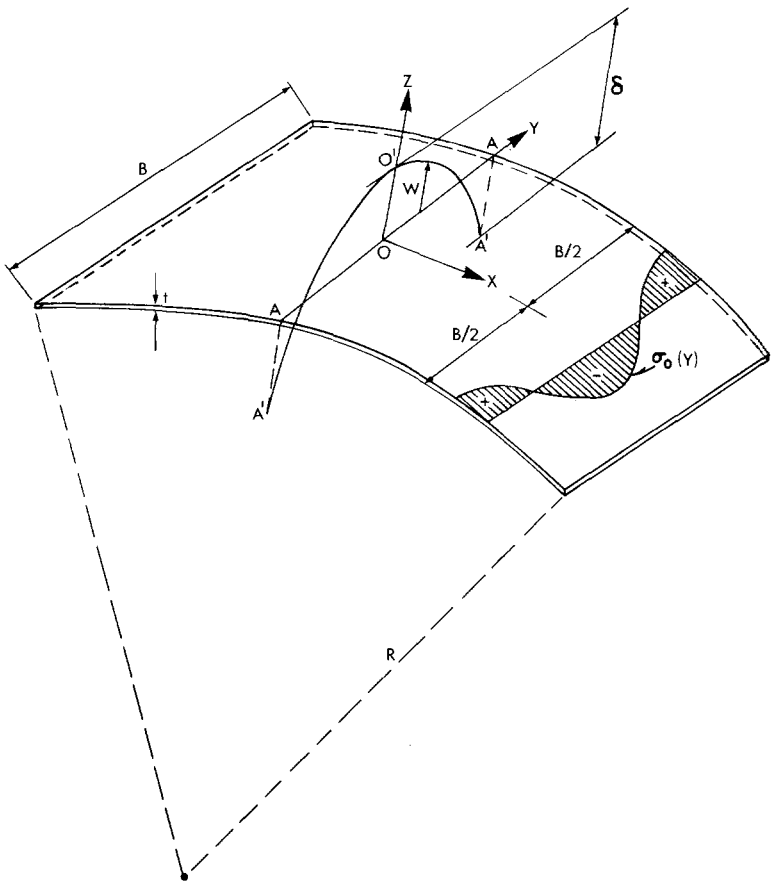

Fig. 1. Bent bandsaw blade and transverse deflected shape

This paper presents an analysis of the relationship between the light-gap δ and the residual stress system and, finally, a discussion of the accuracy of the light-gap technique is presented.

Governing differential equation

Consider again Fig. 1. The differential equation governing the problem and relating the displacement w corresponding to the transverse blade curvature to the residual stress system σ_0 is given by

$$\frac{d^4 w}{dy^4} + \frac{12(1-\nu^2)}{R^2 t^2} w = \frac{-12(1-\nu^2)}{E R t^2} \sigma_0(y) \tag{1}$$

where R is the radius, t the blade thickness, E the modulus of elasticity and ν the Poisson's ratio for the blade.

The problem is very closely related to that of the anticlastic curvature of flat plates and the derivation of Eq. (1), for the case of $\sigma_0(y) = 0$, can be found in the work of several authors [Conway, Nickola 1965; Bellow et al. 1965; Ashwell 1962].

Boundary conditions for Eq. (1) are given by

$$\left.\begin{aligned} \frac{d^2 w}{dy^2} &= \frac{\nu}{R} \\ \frac{d^3 w}{dy^3} &= 0 \end{aligned}\right\} \text{ at } y = \pm B/2 \tag{2}$$

which imply that the edges of the blade are free of stresses.

Homogeneous problem

The homogeneous equation associated with Eq. (1), that is, when $\sigma_0 = 0$, has the general solution

$$w = K_0 \cosh \alpha y \cos \alpha y + K_1 \sinh \alpha y \sin \alpha y \tag{3}$$

where

$$\alpha = \sqrt[4]{\frac{3(1-\nu^2)}{R^2 t^2}} \tag{4}$$

and K_0 and K_1 are arbitrary constants. Only solutions which are symmetrical about $y = 0$ are considered in Eq. (3). If the boundary conditions of Eq. (2) were used to determine the value of the constants K_0 and K_1, the solution thus obtained would correspond to the anticlastic curvature of the bent blade, as shown by Conway and Nickola [1965]. In the general case of a tensioned blade, the homogeneous solution of Eq. (3) must be complemented with particular solutions for the given system of residual stresses $\sigma_0(y)$.

Parabolic residual stresses

For the purpose of studying the solution to Eq. (1) in detail, in the case of a tensioned blade, assume that the residual stresses σ_0 are given by

$$\sigma_0(y) = -\sigma_c + 12\sigma_c \left(\frac{y}{B}\right)^2 \tag{5}$$

where σ_c is the magnitude of the compressive stress at the center of the blade. At the edges $y = \pm B/2$, Eq. (5) gives a tensile stress $\sigma_t = 2\sigma_c$. This parabolic distribution is shown in Fig. 2.

A particular solution to Eq. (1), when Eq. (5) is introduced in its right-hand side, is

$$w_p = \frac{\sigma_c R}{E}\left[1 - 12\left(\frac{y}{B}\right)^2\right] \tag{6}$$

and the general solution can be obtained by adding the result of Eq. (3). The unknown constants K_0 and K_1 can be determined from the pair of boundary condi-

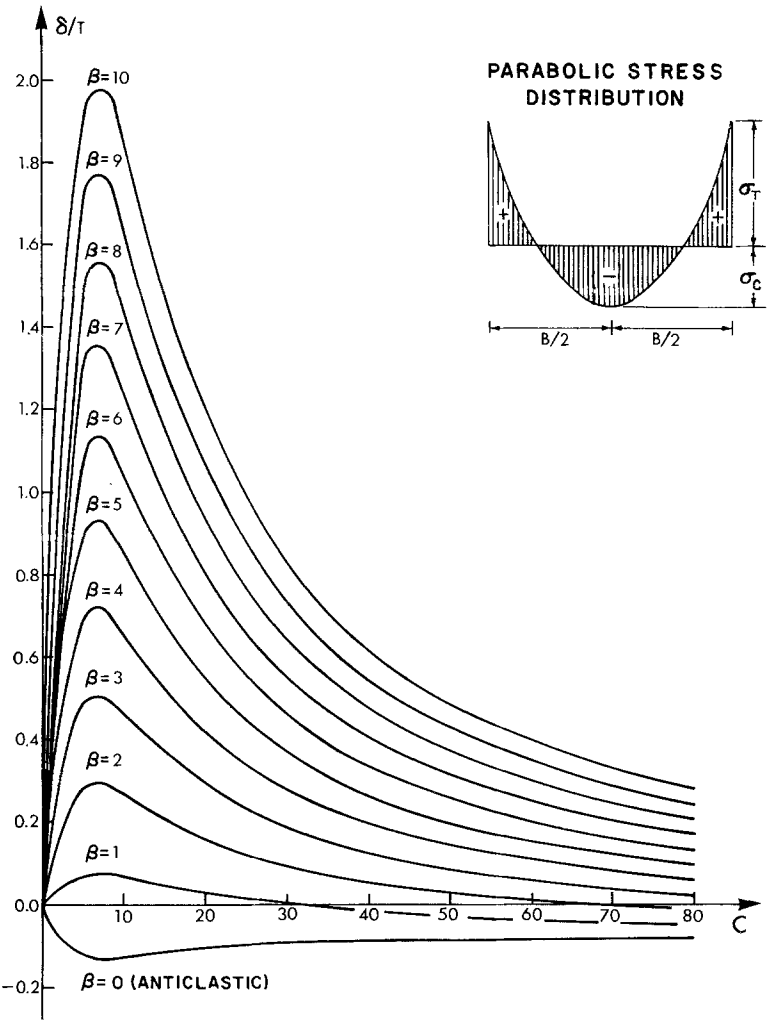

Fig. 2. Light gap for parabolic residual stresses

tions of Eq. (2) and the transverse deflected shape w can finally be expressed as follows:

$$w = \frac{\sigma_c R}{E}\left[1 - 12\left(\frac{y}{B}\right)^2\right] + \\ + \left[\frac{\nu}{R} + \frac{24\,\sigma_c R}{E B^2}\right][\gamma_1 \cosh\alpha y \cos\alpha y + \gamma_2 \sinh\alpha y \sin\alpha y] \qquad (7)$$

where the constants γ_1 and γ_2 are given in the Appendix. The light gap δ is given by

$$\delta = w(0) - w(B/2) \qquad (8)$$

and it may be expressed in nondimensional form as follows:

$$\frac{\delta}{t} = \left[\nu C + 24\frac{\beta}{C}\right]\left[\alpha_1\left(1 - \cosh\frac{\gamma\sqrt{C}}{2}\cos\frac{\gamma\sqrt{C}}{2}\right) - \alpha_2 \sinh\frac{\gamma\sqrt{C}}{2}\sin\frac{\gamma\sqrt{C}}{2}\right] + \\ + 3\beta/C \tag{9}$$

where the constants α_1 and α_2 are given in the Appendix and C, γ and β are defined as

$$\left.\begin{aligned} C &= B^2/R\,t \\ \gamma &= \sqrt[4]{3(1-\nu^2)} \\ \beta &= \frac{\sigma_c}{E}(B/t)^2 \end{aligned}\right\} . \tag{10}$$

Assuming that the distribution of residual stresses is parabolic, therefore, Eq. (9) can be used to determine the light gap δ for any combination of blade geometry and level of tensioning. This equation is plotted in Fig. 2 for different values of the parameters C and β. This figure may be used to calculate δ if the stress σ_c (and thus β) is known, or, vice versa, knowing the light gap δ and the parameter C from the blade geometry, the parameter β (and thus σ_c) can be calculated.

Fig. 3 shows a plot, from Eq. (7), of the relationship between δ and R for a particular blade and a given level of tensioning. The blade considered for this example

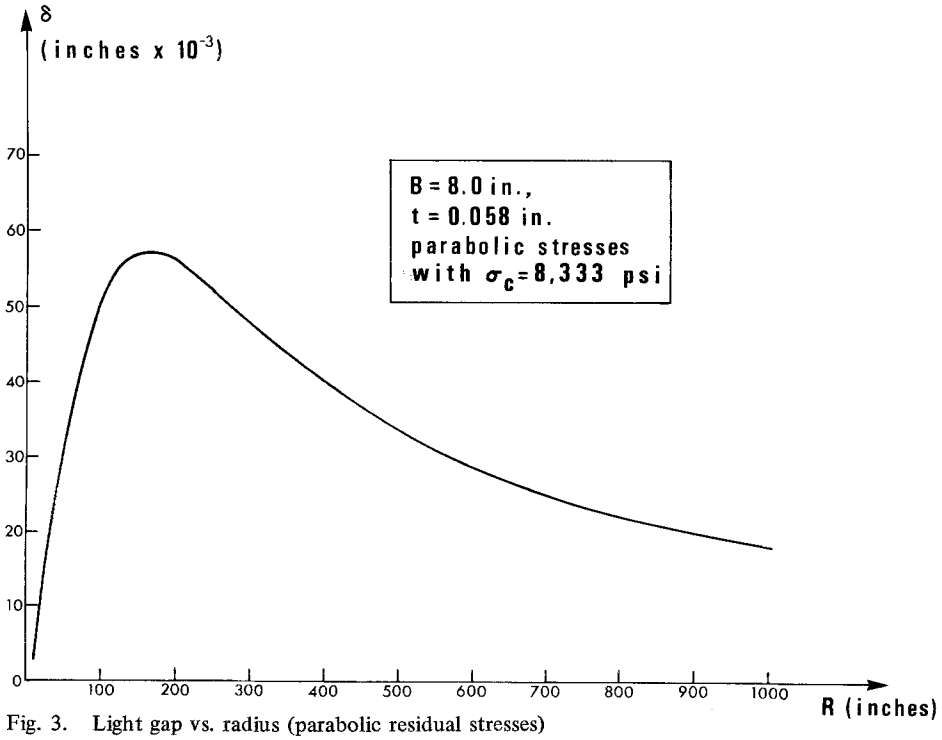

Fig. 3. Light gap vs. radius (parabolic residual stresses)

had the dimensions B = 8.0 in and t = 0.058 in. It was assumed to have been rolled until a compressive residual stress $\sigma_c = 8.333\,\text{lbs/in}^2$ was introduced. A maximum light gap is obtained for a radius of approximately R = 150 in. after which δ decreases approaching zero for infinite radius, that is, for a flat blade. The shape of the curve shown in Fig. 3 compares well with that experimentally obtained by Eklund [1972], although a direct comparison is not possible since it would have to be assumed that the blade used by Eklund had a parabolic distribution of residual stresses.

General case of residual stresses

Consider now the general case where the system of residual stresses is represented, to a satisfactory degree of accuracy, by a Fourier series of the form

$$\sigma_0(y) = \sum_{n=1}^{N} a_n \cos\left(\frac{2n\pi y}{B}\right). \tag{11}$$

A particular solution to Eq. (1) for this general stress system may be taken in the form

$$w_p = \sum_{n=1}^{N} b_n \cos\left(\frac{2n\pi y}{B}\right) \tag{12}$$

with b_n as unknown coefficients. These can be determined by introduction of Eq. (11) and Eq. (12) into Eq. (1). Thus,

$$b_n = -\frac{R}{E}\,\frac{a_n}{1 + 4\left[\frac{n\pi}{\alpha B}\right]^4} \tag{13}$$

with α as given by Eq. (4). Once again, the general solution is found by adding to Eq. (12) the result of Eq. (3). The constants K_0 and K_1 are determined from the pair of boundary conditions of Eq. (2) and the transverse deflected shape w can finally be expressed as follows:

$$w = \sum_{n=1}^{N} b_n \left[\cos\left(\frac{2n\pi y}{B}\right) + \right.$$
$$\left. + (-1)^n \left(\frac{2n\pi}{B}\right)^2 (\gamma_1 \cosh\alpha y \cos\alpha y + \gamma_2 \sinh\alpha y \sin\alpha y)\right] \tag{14}$$

with γ_1 and γ_2 as given in the Appendix. In order to obtain the transverse deflected shape for any residual stress distribution, therefore, it is only required to expand the distribution function in a Fourier series of the form given by Eq. (11), obtain the coefficients a_n and, with Eq. (13), the corresponding coefficients b_n for use in Eq. (14).

It is worthwhile to discuss now the results of Eqs. (13) and (14). Consider a situation where the blade has been rolled in such a manner that a periodic stress system

of the form

$$\sigma_0(y) = a_N \cos\left(\frac{2N\pi y}{B}\right) \tag{15}$$

has been introduced. Further, assume that N is a relatively large number. According to Eq. (13), the amplitude of the deflected shape is inversely proportional to the fourth power of N and, thus, the larger N is, the smaller the light gap. At the same time, however, the amplitude a_N of the stress distribution may be a relatively large number, producing a situation of high stresses that could escape detection by the light gap technique. This effect is shown in Fig. 4, for the same blade considered in plotting Fig. 3. The blade is now assumed bent over a radius R = 30 in., and Fig. 4 shows the results for three different stress distributions $\sigma_0(y)$.

In Case I, a simple cosine distribution (N = 1) is assumed, with an amplitude of 10,000 lbs/in^2. Eq. (14) can be used to determine the corresponding transverse deflected shape and this is shown in Fig. 4. The maximum deflection from the flat

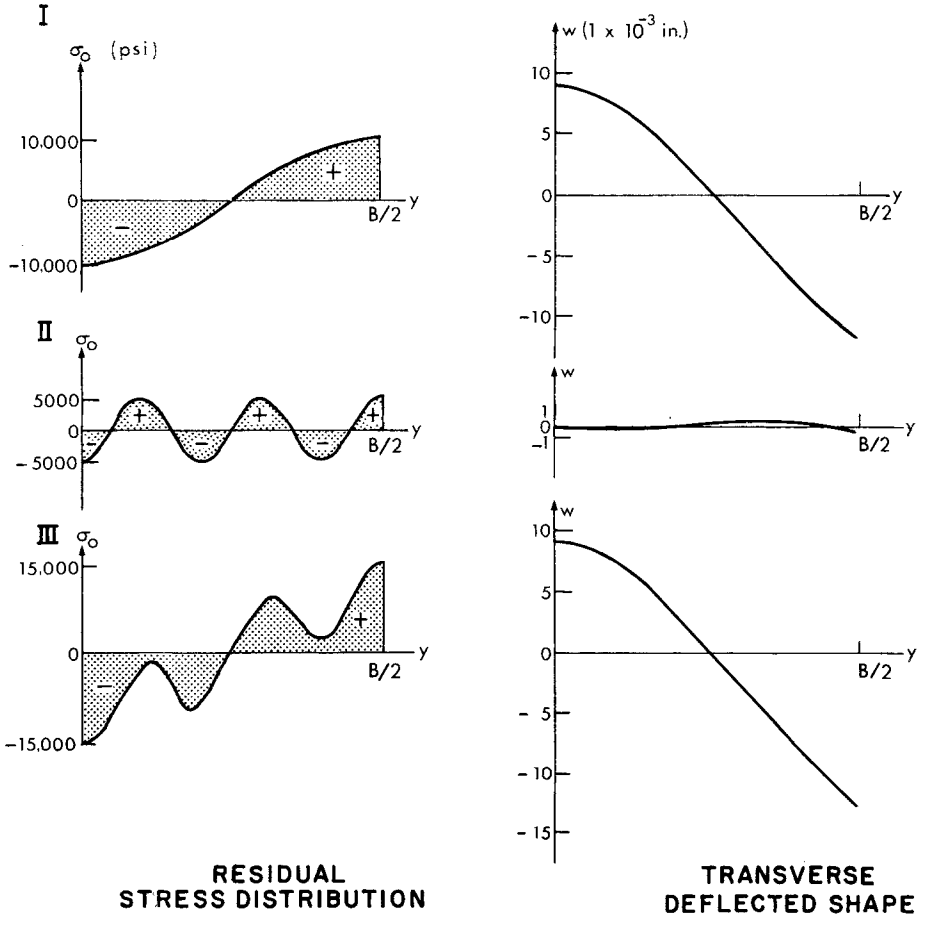

Fig. 4. Sensitivity of transverse deflected shape to variations in residual stresses

occurs at the edges with $w_{max.} = 11.98 \times 10^{-3}$ in. The light gap δ is, on the other hand, $\delta = 21.03 \times 10^{-3}$ in.

Case II shows the results for a cosine distribution with N = 5 and an amplitude of 5,000 lbs/in^2. It is seen that the transverse deflected shape is almost flat, with maximum deflection at the edges of $w_{max.} = 0.68 \times 10^{-3}$ in and a light gap $\delta = 0.76 \times 10^{-3}$ in. Thus, if transverse deflected shapes are measured with an accuracy of 1×10^{-3} in, for example, the shape of Case II could not be distinguished from the flat and a stress of 5,000 lbs/in^2 could go undetected.

Case III is a superposition of the two previous cases. The new stress distribution is, of course, very much different from that of Case I. However, the corresponding transverse deflected shapes are almost identical and could not be differentiated from one another if these shapes are measured with an accuracy of 1×10^{-3} in.

The next section discusses in more detail the accuracy of the method as an estimator of residual stresses and how to set operational requirements to minimize its shortcomings.

Accuracy of the technique

The light gap technique may be used to estimate the residual stresses introduced in the blade by following an indirect approach to the problem. Upon deciding the level of residual stresses desired and the shape of their distribution function, the transverse deflected shape may be calculated by using, for example, Eq. (14). Since the solution to the governing differential equation is unique, conformity of the transverse deflected shape of the blade to the calculated one will ensure that the obtained residual stresses agree with those desired.

The conformity of a measured transverse deflected shape to a desired one is the usual manner in which the light gap technique is used by saw filers, although, in general, no connection is made between this process and the underlying system of residual stresses. It has been found experimentally by Allen [1973] that, if a blade is tensioned until its transverse deflected shape approximately agrees with that corresponding to a parabolic residual stress distribution, sawing accuracy improves over that obtained with blades differently tensioned. According to the previous discussion, however, although the shape is made to agree closely with that of a parabolic stress distribution, the stresses themselves may differ markedly from being parabolic. The question to be answered is then the following: How close would the operator have to come to a desired transverse deflected shape to be within a certain tolerance of the residual stresses corresponding to that desired shape?

To answer this question, consider a residual stress system σ_0 to which corresponds a transverse deflected shape w_0. If the system σ_0 is perturbed by adding the distribution

$$\Delta\sigma = \sum_{n=1}^{N} a_n \cos\left(\frac{2n\pi y}{B}\right) \tag{16}$$

the transverse shape w_0 will change by an amount Δw, which, according to Eq. (14), is given by

$$\Delta w = \sum_{n=1}^{N} b_n \left[\cos\left(\frac{2n\pi y}{B}\right) + \right.$$

$$\left. + (-1)^n \left(\frac{2n\pi}{B}\right)^2 (\gamma_1 \cosh\alpha y \cos\alpha y + \gamma_2 \sinh\alpha y \sin\alpha y) \right] . \qquad (17)$$

By defining the nondimensional variable $\xi = 2y/B$, it is possible to express Eqs. (16) and (17) in the form

$$\Delta\sigma = \sum_{n=1}^{N} a_n g_n(\xi) , \qquad (18)$$

$$\Delta w = \sum_{n=1}^{N} \frac{R}{E} a_n f_n(\xi) \qquad (19)$$

with the functions $g_n(\xi)$ and $f_n(\xi)$ as given in the Appendix. These functions and the amplitudes a_n in Eq. (16) may be considered components of N-dimensional vectors. Thus, if

$$\{F\} = \begin{Bmatrix} f_1(\xi) \\ f_2(\xi) \\ \vdots \\ \vdots \\ f_N(\xi) \end{Bmatrix} ; \qquad \{G\} = \begin{Bmatrix} g_1(\xi) \\ g_2(\xi) \\ \vdots \\ \vdots \\ g_N(\xi) \end{Bmatrix} ; \qquad \{A\} = \begin{Bmatrix} a_1 \\ a_2 \\ \vdots \\ \vdots \\ a_N \end{Bmatrix} ; \qquad (20)$$

Eqs. (18) and (19) become

$$\Delta\sigma = \{G\}^T \{A\} \qquad (21)$$

and

$$\Delta w = \frac{R}{E} \{F\}^T \{A\} \qquad (22)$$

where $\{G\}^T$ and $\{F\}^T$ signify the corresponding transpose vectors of $\{G\}$ and $\{F\}$. To compare the deviations in transverse deflected shape with the corresponding deviations in stresses, the norms of the functions $\Delta\sigma$ and Δw are used. These norms are defined in the following manner [Courant, Hilbert 1953]:

$$\| \Delta\sigma \| = \tfrac{1}{2} \int_{-1}^{+1} (\Delta\sigma)^2 \, d\xi , \qquad (23)$$

$$\| \Delta w \| = \tfrac{1}{2} \int_{-1}^{+1} (\Delta w)^2 \, d\xi , \qquad (24)$$

and can be calculated by using Eqs. (21) and (22). That is,

$$\| \Delta\sigma \| = \tfrac{1}{2} \{A\}^T \left[\int_{-1}^{+1} \{G\} \{G\}^T \, d\xi \right] \{A\} , \qquad (25)$$

$$\|\Delta w\| = \tfrac{1}{2} \{A\}^T \left[\int_{-1}^{+1} \{F\} \{F\}^T \, d\xi \right] \{A\} \cdot \left(\frac{R}{E}\right)^2 . \tag{26}$$

The ratio of the norms $\|\Delta \sigma\|$ and $\|\Delta w\|$ can then be expressed as

$$\frac{\|\Delta \sigma\|}{\|\Delta w\|} = \left(\frac{R}{E}\right)^2 \frac{\{A\}^T [M] \{A\}}{\{A\}^T \{A\}} \tag{27}$$

where [M] is the matrix

$$[M] = \int_{-1}^{+1} \{F\} \{F\}^T \, d\xi . \tag{28}$$

It can be shown that, for any vector $\{A\}$,

$$\lambda_{min} \leqslant \frac{\{A\}^T [M] \{A\}}{\{A\}^T \{A\}} \leqslant \lambda_{max} \tag{29}$$

where λ_{max} and λ_{min} are, respectively, the largest and smallest eigenvalues of the matrix [M]. If the square root of the corresponding norm is regarded as the measure of the deviations from the desired shape and stress distributions and these measures are defined as E_w and E_σ, respectively, it is obtained from Eqs. (27) and (29) that

$$\left(\frac{E}{R}\right) \frac{E_w}{\sqrt{\lambda_{max}}} \leqslant E_\sigma \leqslant \left(\frac{E}{R}\right) \frac{E_w}{\sqrt{\lambda_{min}}} . \tag{30}$$

For all possible forms of the perturbation $\Delta \sigma$, that is, for all vectors $\{A\}$, the deviation E_σ between stress distributions and the deviation E_w between the corresponding transverse deflected shapes will satisfy the unequality of Eq. (30). It is important to note that the bounds obtained for E_σ in Eq. (30) are given in terms of eigenvalues of the matrix [M] which was assumed to be N x N. If the function $\Delta \sigma$ contains terms with frequency larger than N, the matrix [M] will change and its eigenvalues will naturally change. The upper bound in Eq. (30) is of importance, for, if it is desired that the deviation E_σ in stresses do not exceed a prescribed tolerance T_σ, the deviation E_w in transverse deflected shape must not exceed the value

$$T_w = \left(\frac{R}{E}\right) \sqrt{\lambda_{min}} \, T_\sigma . \tag{31}$$

Since the smallest eigenvalue of the matrix [M] depends on N, the tolerance of Eq. (31) must be referred to as "with respect to a given N". Fig. 5 shows the dependence of $\sqrt{\lambda_{min}}$ on the parameters C and N. It is seen that, as N increases, $\sqrt{\lambda_{min}}$ approaches zero for all values of C, implying, from Eq. (31), that very precise tolerances T_w are required to detect stress deviations T_σ with relatively high frequency components. This effect is the same as that discussed in the previous section in connection with large N.

As an example, consider the blade used for plotting Fig. 3. Bent over a radius R = 30 in., and assuming that it has been rolled until a parabolic stress distribution has been introduced with σ_c = 8,333 lbs/in^2, Fig. 3 shows that the light gap is

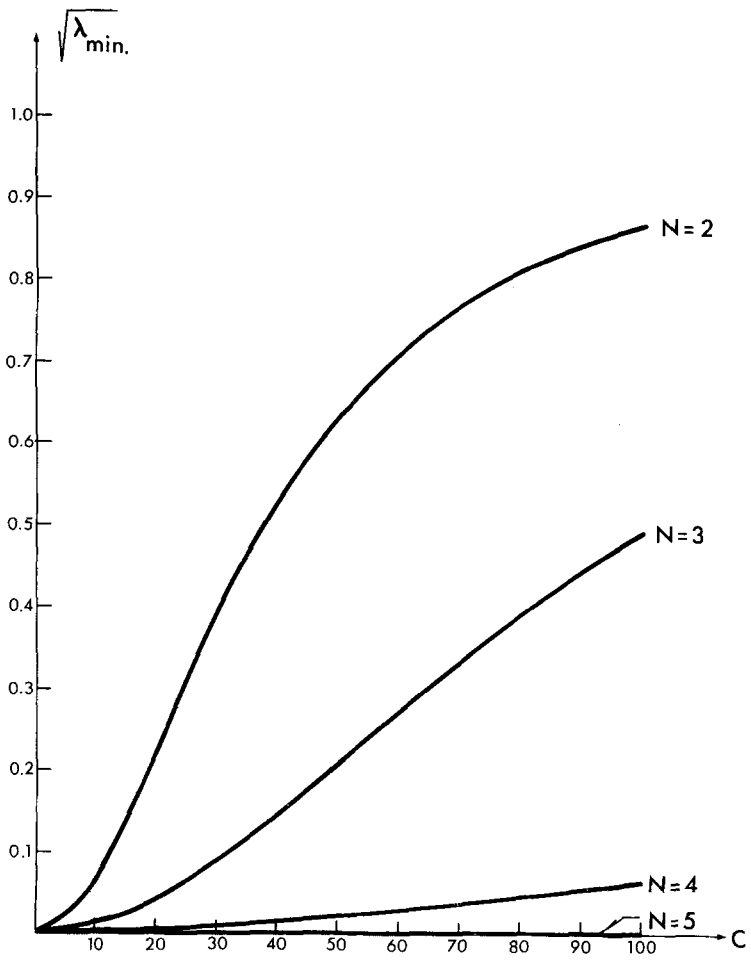

Fig. 5. Tolerance factor $\sqrt{\lambda_{min}}$

$\delta = 0.018$ in. The corresponding value of C is 36.78. Table 1 shows the tolerances T_w for different values of N and for a tolerated stress deviation, from the parabolic distribution, of $T_\sigma = 2{,}500\,\text{lbs/in}^2$. For example, any stress deviation with N up to N = 2 will be less than or equal to $2{,}500\,\text{lbs/in}^2$ if the shape for the parabolic distribution is approached to within $T_w = 0.001225$ in. But stress deviations larger than

Table 1. Required tolerances[1]

N	$\sqrt{\lambda_{min}}$	T_w (inches x 10^{-3})
2	0.490	1.225
3	0.125	0.313
4	0.015	0.038

[1] B = 8.0 in; t = 0.058 in; R = 30.0 in; E = 30×10^6 lbs/in^2; stress tolerance $T_\sigma = 2{,}500\,\text{lbs/in}^2$.

2,500 lbs/in^2 would produce transverse shapes differing from that of the parabolic stress distribution by less than 0.001225 in. if N = 4. Accordingly, to be able to detect stress deviations larger than 2,500 lbs/in^2 when N = 4, the tolerance T_w must be reduced, in this case, to T_w = 0.000038 in. This number would be reduced even further if stress deviations with N = 6 or larger were to be considered.
It is obvious then that the method may be used within rather narrow bounds as an estimator of residual stresses. Eq. (31) may be used to set a given tolerance T_w after a decision has been made on the number N to be protected against and the stress difference T_σ to be tolerated, but it is important to keep in mind that an indiscriminate rolling schedule may induce stresses with components of large magnitude and relatively high frequency and that these would be almost undetectable by the light gap technique.

Conclusions

The relationship between residual stresses induced by cold rolling of bandsaw blades and the transverse deflected shape obtained when a blade is bent over a given radius has been studied. It has been shown that, while this transverse shape is uniquely related to the distribution of residual stresses, two different shapes may be very close to each other while the corresponding stress distributions may be far apart. This is a characteristic of the light gap technique which reduces its accuracy as an estimator of residual stresses. In particular, it has been shown that the combination high frequency-high amplitude in a periodic stress distribution could be almost undetectable by the technique. The method may be improved by adjusting the tolerance with which the saw filer approaches a desired shape during tensioning, and a procedure for computing this tolerance has been presented. Nevertheless, the light gap technique cannot be considered a reliable estimator of residual stresses and other non-destructive, more accurate methods, should be investigated for application to bandsaw blades.

Appendix

$$\gamma_1 = \frac{\sinh\frac{\alpha B}{2}\cos\frac{\alpha B}{2} - \cosh\frac{\alpha B}{2}\sin\frac{\alpha B}{2}}{\alpha^2(\sinh\alpha B + \sin\alpha B)},$$

$$\gamma_2 = \frac{\sinh\frac{\alpha B}{2}\cos\frac{\alpha B}{2} + \cosh\frac{\alpha B}{2}\sin\frac{\alpha B}{2}}{\alpha^2(\sinh\alpha B + \sin\alpha B)},$$

$$\alpha_1 = \frac{\sinh\frac{\gamma\sqrt{C}}{2}\cos\frac{\gamma\sqrt{C}}{2} - \cosh\frac{\gamma\sqrt{C}}{2}\sin\frac{\gamma\sqrt{C}}{2}}{\gamma^2 C(\sinh\gamma\sqrt{C} + \sin\gamma\sqrt{C})},$$

$$\alpha_2 = \frac{\sinh\frac{\gamma\sqrt{C}}{2}\cos\frac{\gamma\sqrt{C}}{2} + \cosh\frac{\gamma\sqrt{C}}{2}\sin\frac{\gamma\sqrt{C}}{2}}{\gamma^2 C(\sinh\gamma\sqrt{C} + \sin\gamma\sqrt{C})},$$

$$f_n(\xi) = b_n^*\left[\cos(n\pi\xi) + (-1)^n 4n^2\pi^2\left(\alpha_1\cosh\frac{\gamma\sqrt{C}\xi}{2}\cos\frac{\gamma\sqrt{C}\xi}{2} + \right.\right.$$

$$\left.\left. + \alpha_2\sinh\frac{\gamma\sqrt{C}\xi}{2}\sin\frac{\gamma\sqrt{C}\xi}{2}\right)\right],$$

$$g_n(\xi) = \cos(n\pi\xi),$$

and

$$b_n^* = -\frac{1}{1 + 4\left[\frac{n\pi}{\gamma\sqrt{C}}\right]^4}.$$

References

Allen, F. E. 1973. Quality control in the timber industry. Austral. Forest Ind. J. 39 (8): 30–35

Aoyama, T. 1970. Tensioning of band saw blade by rolls. Part II. J. Jap. Wood Res. Soc. 16: 376–381

Aoyama, T. 1971. Tensioning of band saw blade by rolls. Parts III and IV. J. Jap. Wood Res. Soc. 17: 188–202

Aoyama, T. 1974. Tensioning of band saw blade by rolls. Part V. J. Jap. Wood Res. Soc. 20: 523–527

Ashwell, D. G. 1962. Nonlinear problems. In Flugge, W. (Ed.) Handbook of engineering mechanics. New York: McGraw Hill, 45–11

Bellow, D. G.; Ford, G.; Kennedy, J. S. 1965. Anticlastic behavior of flat plates. Exp. Mech. 5 (7): 227–232

Conway, H. D.; Nickola, W. E. 1965. Anticlastic action of flat sheets in bending. Exp. Mech. 5 (4): 115–119

Courant, R.; Hilbert, D. 1953. Methods of mathematical physics, Vol. I. New York: Interscience, 49

Eklund, U. 1972. Ljusspalten som matt pa bandsagbladets strackning. Swed. For. Prod. Res. Lab., STFI, Publ. 227 (32)

Szymani, R.; Mote, C. D. Jr. 1974. A review of residual stresses and tensioning in circular saws. Wood Sci. Technol. 8: 148–161

(Received July 16, 1975)

Ricardo O. Foschi
Western Forest Products Laboratory,
Canadian Forestry Service,
Department of the Environment,
6620 NW Marine Dr.,
Vancouver, B.C., Canada